Received: 7 October 2019 | Revised: 25 November 2019 | Accepted: 8 December 2019

DOI: 10.1002/aoc.5440

Applied Organometallic Chemistry WILEY

FULL PAPER

Iron oxide magnetic nanoparticles supported on amino propyl-functionalized KCC-1 as robust recyclable catalyst for one pot and green synthesis of tetrahydrodipyrazolopyridines and cytotoxicity evaluation

Sajjad Azizi | Jafar Soleymani | Mohammad Hasanzadeh

Pharmaceutical Analysis Research Center and Faculty of Pharmacy, Tabriz University of Medical Sciences, Tabriz, Iran

Correspondence
Mohammad Hasanzadeh, Pharmaceutical Analysis Research Center and Faculty of Pharmacy, Tabriz University of Medical Sciences, Tabriz, Iran.
Email: mhmmd_hasanzadeh@yahoo.com; hasanzadehm@tbzmed.ac.ir

In this study, paramagnetic dendritic fibrous nano-silica functionalized by aminopropyltriethoxysilan (Fe_3O_4@KCC-1-nPr-NH_2) was synthesized using a novel hydrothermal protocol and used as a highly efficient, recyclable and heterogeneous nanocatalyst for the synthesis of a wide range of tetrahydrodipyrazolopyridines derivatives (**5a-5 m**). The influence of different reaction parameters, such as the effects of solvent, temperature, time and concentration of catalyst for the synthesis of tetrahydrodipyrazolopyridine (2a) were studied. This catalyst could be reused for ten consecutive recycles without any considerable loss in its catalytic activity. This novel synthesis method offers some advantages including short reaction time, high yield and simple work-up procedure. Finally, the newly synthesized tetrahydrodipyrazolopyridines derivatives (**5a-5f**) were characterized by ^{1}H and ^{13}C NMR, IR and CHN.

KEYWORDS

bioactive compounds, fibrous nano-silica, magnetic nanoparticle, nano-catalyst, tetrahydrodipyrazolopyridines

1 | INTRODUCTION

Pyrazolopyridines represent a well-known scaffold in various bioactive compounds and have numerous pharmacological properties. These compounds exhibit important biological properties, including antibacterial,[1,2] antimicrobial,[3,4] antifungal,[5] antitumor,[6] anti-virus,[7] anti-Leishmania,[8] HIF 1-αprolyl hydroxylase inhibitors,[9] B-Raf ^{V600E3} inhibitors,[10] protein kinase inhibitors,[11] PDE4B inhibitors,[12] dopaminergic properties[13] and cancer cell growth inhabitation activities.[14] The main problems for the synthesis of pyrazolopyridine compounds are long reaction times, utilize of non-reusable and toxic catalyst and use of particular conditions. Therefore, looking for simple and efficient methods for the synthesis of pyrazolopyridines is essential. For these reasons, Multicomponent reactions (MCRs) are specially well suited for variety-oriented synthesis.[15,16] Thus; the synthesis of pyrazolopyridines by the multicomponent reactions with a suitable catalyst could enhance their efficiency from ecological points of view.

Several kinds of catalysts have been used to advance the reactions using MCRs (multicomponent reactions), such as acetic acid,[17] carbonaceous material (C-SO_3H),[18] p- TSA[19] and L-Proline.[20] In recent years, the use of nanocatalysts has increased quickly and caused in the advancement of several active and capable

nanocatalysts for various procedures.[21–24] These materials have several advantages over formal catalysts, such as excellent activity and high stability. In addition, metal nanoparticles with a superior support provides a large area for the discovery of novel, highly active nanocatalysts for significant and challenging reactions, which also propose the more advantage of recyclability. Moreover, surface functionalized mesoporous systems have appeared as one of the most significant research areas in the concerning of advanced functional materials. Particularly, Polshettiwar et al reported fibrous nanosilica (KCC-1), with the high surface area (typically >700 m^2/g), broad pore size distribution, large pore sizes,[25,26] ease of surface modification, low density, stability and low toxicity with good biocompatibility.[9,11,12] This Dendritic fibrous nanosilica showed special activities in vast fields such as heterogeneous catalysis,[27] gas capture, solar energy harvesting, energy storage,[28] medical diagnosis, targeting of drugs,[7,29–31] DNA adsorption [26] drug delivery applications,[32] bio sensing [33] and CO_2 Mitigation.[34]

In this study, we reported the use of Fe_3O_4@KCC-1-nPr-NH_2 as an advanced novel nanocatalystis for the synthesis of tetrahydrodipyrazolopyridine (**5a-m**) compounds by multicomponent reaction of aromatic aldehydes, hydrazinehydrate (or phenylhydrazinehydrate), ethyl acetoacetate (or diethylmalonate) and ammonium acetate under reflux conditions in ethanol as a solvent (Scheme 1). Finally, we investigated the anti-cancer activity of novel synthesized pyrazolopyridines scaffold (**5a-5f**) by MTT assay.

In the present work, Fe_3O_4@KCC-1-npr-NH_2 was applied as a novel catalyst for synthesis of sulfonamide derivatives. The use of this novel dendritic nanocatalyst has some important advantages including produce the products in excellent yields, simple recovery and reusability of catalyst for ten times without significant decrease in activity and easy separation by external magnet. Also this method has short reaction time and simple work-up procedure. According to the obtained results, proposed method gave the product in high yield in comparison with other reports.

2 | EXPERIMENTAL

2.1 | Materials and methods

All of materials and solvents were purchased from Merck, Sigma Aldrich and Fluka in high purity and used without further purification. Melting points were measured in open capillariesusing an Electrothermal MEL-TEMP apparatus (model 9200). FTIR spectra were obtained with a Bruker Tensor 27 spectrometer; υ in cm^{-1} in the transmission mode in spectroscopic grade KBr tablets for all the powders. The ^1H and ^{13}C NMR spectra were observed with a Bruker Spectrospin Avance 400 spectrometer operating at 400 MHz and 100 MHz respectively. Elemental analyses for C, H, and N were performed using a Heraeus CHN–O-Rapid. X-ray diffraction (XRD) patterns of KCC-1 based materials were recorded by Siemens D 5000 X-Ray diffractometer (Texas, USA) with a Cu K_α anode (λ = 1.54 A°) operating at 40 kV and 100 mA. The Scanning Electron Microscopy (SEM) images and Energy Dispersive X-Ray (EDX) were recorded with FEG-SEM MIRA3 TESCAN, Czech Republic) at 1000 kV. Transmission Electron Microscopy (TEM) analysis was conducted on a Carl Zeiss LEO 906 electron microscope operated at 100 kV (Oberkochen, Germany). Brunauer–Emmett–Teller (BET) was recorded by Micromeritics NOVA 2000 (Florida, USA) apparatus at 77 K using nitrogen as the adsorption gas. The particle size distribution and zeta potential values were determined using Malvern particle size analyzer (Malvern, UK). The purity determination of the products and reaction monitoring were accomplished by TLC on silica gel poly gram SILG/UV 254 plates. MCF 7 and HT-29 were purchased from the national cell bank of Iran (NCBI) where is located in the Pasteur (Tehran, Iran).

2.2 | General procedure for the synthesis of Fe_3O_4 magnetic nanoparticles

The synthesis procedure of hydrophilic nanoparticles Fe_3O_4 is explained as follows:

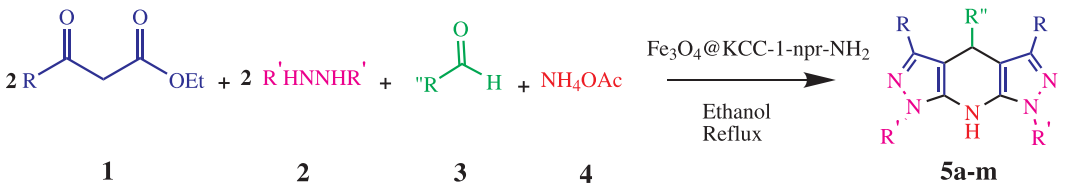

SCHEME 1 Synthesis of tetrahydrodipyrazolopyridines (5a-m) in the presence of KCC-1-NH_2- Fe_3O_4@KCC-1-npr-NH_2 NPs

Briefly, $FeCl_3.6H_2O$ (3.25 g) was dispersed along with sodium acetate (NaAc, 6.0 g) and trisodium citrate (1.3 g) in the ethylene glycol (100 ml) with stirring. The collected yellow solution was transferred in a Teflon-lined stainless-steel autoclave with 200 ml capacity and the heating process of autoclave was continued about 10 hr at 200 °C. After cooling at room temperature the black product was rinsed several times with water and ethanol.[35]

2.3 | General procedure for the synthesis of Fe_3O_4@KCC-1 magnetic nanoparticles

At first stage the mixture of 0.1 g of the Fe_3O_4 and 1.8 g of urea in 15 ml of water were sonicated about 30 minutes. Then cetyl trimethyl ammonium bromide (CTAB) 1.0 g, n-butyl alcohol 1.0 g and cyclohexane 20 g were added respectively and stirred for 30 minutes. At this stage tetraethyl orthosilicate (TEOS) (1.00 g) was added drop wise and stirred with mechanical stirrer for 24 hr. at 70 °C. Then, the product was washed with ethanol and water a few times for further process and dried in vacuum at 80 °C for 12 hr and finally calcined at 550 °C for 5 hr in air to remove CTAB as template.

2.4 | General procedure for the synthesis of nanocatalyst (Fe_3O_4@ KCC-1-npr-NH_2)

For this purpose, Fe_3O_4@KCC-1 (0.2 g) added in toluene (100 ml) and sonicated for 30 min. Then, (3-aminopropyl) triethoxysilane (APTES) (500 μL) were added in the mixture and the solution was refluxed for 24 hr under N_2. After that, the product was centrifuged, and was further purified by washing with ethanol and toluene several times and dried at 80 °C. Scheme 2 showes synthesize procedure of Fe_3O_4@ KCC-1-npr-NH_2 as an advanced nanocatalyst.

2.5 | General procedures for the synthesize of tetrahydrodipyrazolopyridine (5a-m)

A mixture of ethyl acetoacetate (or diethylmalonate) (2 mmol) (1) and hydrazine hydrate (or phenyl hydrazine) (2.0 mmol) (2) and Fe_3O_4@ KCC-1-NH_2 (0.1 mg) in EtOH (3 ml) was magnetically stirred for 5 min at 25 °C followed by addition of aromatic aldehyde (1.0 mmol) (3) and ammonium acetate (4.0 mmol) (4). The reaction mixture was heated under reflux conditions for 5–30 min and then cooled to 25 °C. Then, the mixture monitored by TLC and after completion of the reaction, the catalyst Fe_3O_4@ KCC-1-NH_2 MNPs were separated by strong external magnet. The obtained precipitate was washed with EtOH to afford the pure product and then dried well under vacuum pump. As can be seen, the synthesis of derivative (5f) shows different chemical structure (scheme 3).

2.6 | Cell culture and biological tests

2.6.1 | General cell culture procedure

The MCF 7 and HT 29 cancer cells were cultured in Roswell Park Memorial Institute 1640 (RPMI) media

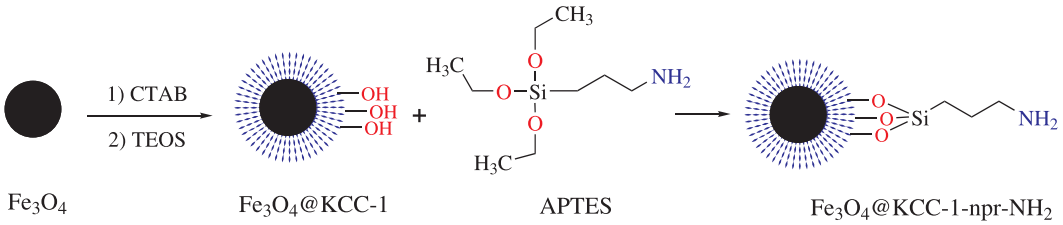

SCHEME 2 Schematic for the synthesis of Fe_3O_4@KCC-1-npr-NH_2

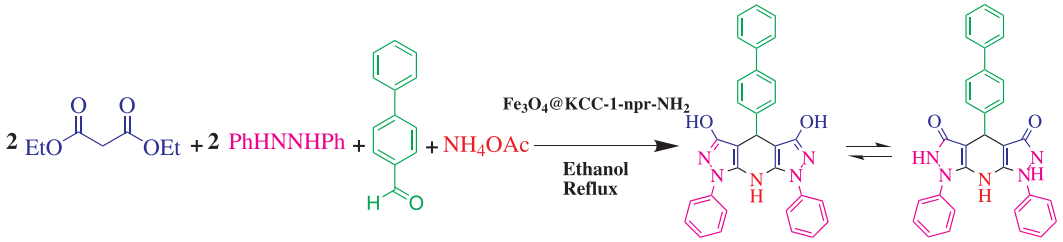

SCHEME 3 Balance of tetrahydrodipyrazolopyridines (5f)

supplemented with 10% FBS and 1% penicillin and streptomycin at 37 °C under 5% CO_2. The cells were washed with phosphate buffer solution (PBS) to remove the excess RPMI and then the cells were treated with trypsin–EDTA solution and incubated for 5 min at 37 °C under 5% CO_2 to separate the cell from the flask bottom surface. Then, the separated cancer cells were transferred to a tube and centrifuged to wash out excess trypsin–EDTA. Finally, the separated cells were resuspended to the fresh RPMI medium.

2.6.2 | MTT assay

Cell viability of MCF 7and HT 29 cancer cells were tested by adding of 1.0×10^4 cells per each well a 96-well texture plate. Afterwards, the cancer cells were incubated for about 24 hr to grow and cover at least 40% of each well. Then, the wells were treated with different concentrations of the 1,4-dihydropyridines and incubated for 48 hr. Next, the wells were washed with PBS buffer solution, and subsequently 20 μL of MTT (2.5 $mg.ml^{-1}$) reagent and 180 μL RPMI refresh media were added to each well and incubated for 4 hr at 37 °C under 5% CO_2. Afterwards, the RPMI media was replaced by 200 μL of DMSO and incubated for 0.5 rh. Finally, the absorbance of the wells was measured at 570 nm.[36]

3 | RESULTS AND DISCUSSION

The synthesis of Fe_3O_4@ KCC-1-NH_2 magnetic nanocatalyst involved several stages (Scheme 3). To investigate of the morphology of Fe_3O_4@KCC-1-NH_2 MNPs, the FESEM images were recorded (Figure 1a). Moreover, the structure and size of the Fe_3O_4@ KCC-1-NH_2 MNPs were evaluated utilizing transmission electron microscopy (TEM). As shown in Figure 1b, the uniform fibers of the magnetic KCC-1 with high surface area have several Si-OH groups that could grows from the center to outside. The TEM images revealed the porous, fibrous and dendritics form of the magnetic nanomaterials which the fibrous system is as a result of using the CTAB for the MNPs design while the fibrous-sphere reveals the formation of KCC-1 based MNPs. The size of the Fe_3O_4 MNPs is about 15 nm. As can be seen in Figure 1 (a and b), the Fe_3O_4@KCC-1-NH_2 MNPs had a constant particle size range of 20 nm. EDX results indicate the atomic structure of the produced compound that the KCC-1 is composed only with Si and O. Though, the carbon is arising from the SEM grid and CTAB as a pattern agent. Moreover, functionalization of KCC-1 with APTES, the weight percent of N, O and C are increased which confirmed successful functionalization of KCC-1 by n-pr-NH_2 (Figure S1).

The powder X-ray diffraction patterns of Fe_3O_4@KCC-1-NH_2 are shown in Figure S2. The XRD pattern of Fe_3O_4@KCC-1-NH_2 NPs was performed from 5.0° (2θ) to 100.0° (2θ) to investigate the crystallinity of the produced nanomaterial in order to obtain additional information about their molecule structures. As can be observed, sample possess the diffraction peaks at (220), (311), (400), (422), (511) and (440), which are in similarity with the data for a standard Fe_3O_4 sample, as reported in the work. The wide peak between 20° and 30° is related to the amorphous silica and proved the effective coating of the silica on Fe_3O_4 core. It is important to point out that the XRD templates of the Fe_3O_4@KCC-1-NH_2 NPs is similar to the fibrous mesoporous silica with Fe_3O_4 core.[37]

The N_2 adsorption–desorption isotherms of Fe_3O_4 @ KCC-1-NH_2 are shown in (Figure S3 (c)). The BET and BJH analyses of the Fe_3O_4 @ KCC-1-NH_2 MNPs were used to determine the porous essence of the synthesized nanocatalyst Figure 3S. (c). The specific surface area and porosity of the nanomaterials were determined using the adsorption isotherm and calculated by BET. Also, BJH technique was used to evaluate the pore volume of the KCC-1, KCC-1-NH_2 and Fe_3O_4 @ KCC-1-NH_2 (Figure 3S.

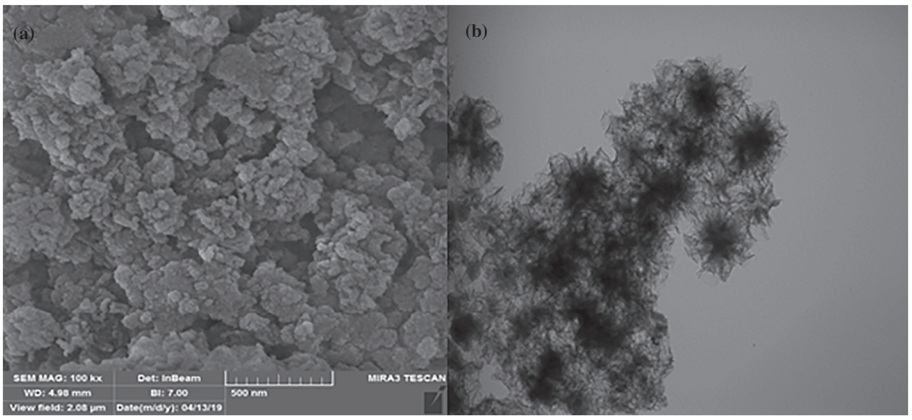

FIGURE 1 FE-SEM (a) and TEM (b) images of Fe_3O_4@KCC-1-npr-NH_2

(a-c)). The surface area of KCC-1, KCC-1-NH_2 and Fe_3O_4@ KCC-1-npr-NH_2 was observed about 617, 367 and 87 m^2 g^{-1}, and also the average pore size is 5.8 nm. The pore volumes, pore size, and surface area of KCC-1, KCC-1-NH_2 and Fe_3O_4 @ KCC-1-NH_2 are clearly proved by the reported results.[33,38,39]

Zeta potentials of Fe_3O_4 @ KCC-1-NH_2 was checked at pH 7.5 to control the surface charge to determine the possible surface modification. The zeta potential of the Fe_3O_4@KCC-1@NH_2 shows positive charges which verify the anchoring amine and Fe_3O_4 groups on the surface of the fibrous system, respectively.[39] Also, DLS result of the Fe_3O_4@KCC-1-NH_2 approves again the successful functionalization of KCC-1 with npr-NH_2 and Fe_3O_4 witch the first peak related to Fe_3O_4 and the second peak related to KCC-NH_2 (Figure S4).

After characterization of Fe_3O_4@ KCC-1-npr-NH_2 the catalytical performance of this nanomatrial was tested for the synthesis of tetrahydrodipyrazolopyridines. In order to optimize the multicomponent reaction conditions and obtain well catalytic activity, the synthesis of tetrahydrodipyrazolopyridine was used as a model, and investigated under different reaction parameters including amount of the catalyst, time, temperature, and solvent type. Initially, the effect of solvent on the synthesis of tetrahydrodipyrazolopyridine compounds using the Fe_3O_4@KCC-1-npr-NH_2 as a nanocatalyst was investigated. It is obtained that; the solvent type does affect the performance of the nanocatalyst. For example, cyclohexane, n-Hexane and CCl_4, which are non-polar solvents, gave tetrahydrodipyrazolopyridine in a lower yield than other solvents (Table 1, entry 5–7). Also, some aprotic polar solvents including THF, CH_3CN, CH_2Cl_2, $CHCl_3$, DMF, EtOAc, toluene and DMSO lead to low efficiency (Table 1, entry 8–15). But, the protic solvents improved reaction performance. Methanol and iPrOH gave tetrahydrodipyrazolo pyridine in average yields (Table 1, entries 16 and 17). In contrast, the utilize of water caused in an increased yield of 76%, while the yield was considerably increased up to 98% when ethanol was used as an organic solvent in the presence of Fe_3O_4@KCC-1-NH_2 MNPs. Also, it is found that conventional heating under reflux conditions in ethanol as a solvent (Table 1) in 5–30 min in the presence 0.0001 g of Fe_3O_4@KCC-1-NH_2 is optimum condition for the synthesize of tetrahydrodipyrazolo pyridines. The role of temperature in the synthesis of tetrahydrodipyrazolo pyridine in the presence of Fe_3O_4@KCC-1-NH_2 MNPs as the catalyst was evaluated, also. In this case, the tetrahydrodipyrazolo pyridines were obtained with excellent isolated yield at 76 °C and results clearly indicated that reaction completion is related to reaction temperature. The optimum temperature for this reaction was at 76 °C. The high temperatures lead to alterations in the efficiency of the reaction (Table 1, entry 1 and 2). Finally, the amount of nanocatalyst on the reaction efficiently was tested. According to obtained results, the variation in the Fe_3O_4@KCC-1-NH_2 MNPs amount had a key role on the reaction efficiency. The optimum amount of Fe_3O_4@KCC-1-NH_2 MNP was 0.1 mg, which obtained the desired product in 98% yields (Figure 2). It is important to point out that, we could achieve to excellent yields of tetrahydrodipyrazolo pyridine synthesize using this nanocatalyst, in 5–30 min (Figure 3).

TABLE 1 The effect of solvent and temperature for the synthesis of tetrahydrodipyrazolo pyridine

Entry	Solvent	Temp. (°C)	Yield (%)
1	EtOH	r.t.	71
2	EtOH	reflux	98
3	H_2O	r.t.	50
4	H_2O	reflux	76
5	Cyclohexane	r.t.	14
6	n-Hexane	r.t.	18
7	CCl_4	r.t.	21
8	THF	r.t.	33
9	CH_3CN	r.t.	40
10	CH_2Cl_2	r.t.	32
11	$CHCl_3$	r.t.	42
12	DMF	r.t.	20
13	EtOAc	r.t.	44
14	Toluene	r.t.	33
15	DMSO	r.t.	39
16	Methanol	r.t.	60
17	i-PrOH	r.t.	52

Reaction conditions: ethyl acetoacetate (or diethylmalonate) (2 mmol), hydrazine hydrate (or phenyl hydrazine) (2.0 mmol), aromatic aldehyde (1.0 mmol) and ammonium acetate (4.0 mmol), Fe3O4@ KCC-1-npr-NH2 (0.1 gm), EtOH (5 ml), under reflux conditions for 30 min. Isolated yield (%).

To further investigate the efficiency of the nanocatalyst, we compared the catalytic performance of the newly nanocatalyst with different control experiment and the results are shown in Table 2. Originally, a standard reaction was accomplished using KCC-1, KCC-1-NH_2, Fe_3O_4 and KCC-1-Fe_3O_4; and the results confirmed that the desired product was not formed (Table 2, entries 1 and 4) after 1 hr of reaction time in any amount. When, Fe_3O_4@KCC-1-NH_2 was used as the nanocatalyst, a reaction was performed and completed (Table 2, entries 5).

Ultimately, the reaction conditions were optimized, and to carry out this approach, we specially evaluated this methodology utilizing phenyl hydrazine

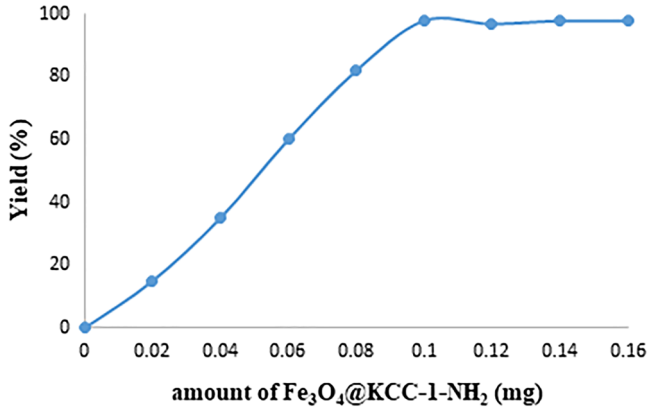

FIGURE 2 Optimization of the conditions for synthesis of tetrahydrodipyrazolo pyridines: ethyl acetoacetate (or diethylmalonate) (2 mmol), hydrazine hydrate (or phenyl hydrazine) (2.0 mmol), aromatic aldehyde (1.0 mmol) and ammonium acetate (4.0 mmol), Fe_3O_4@ KCC-1-npr-NH_2 (0.1 mg), EtOH (5 ml), under reflux conditions, 1 hr

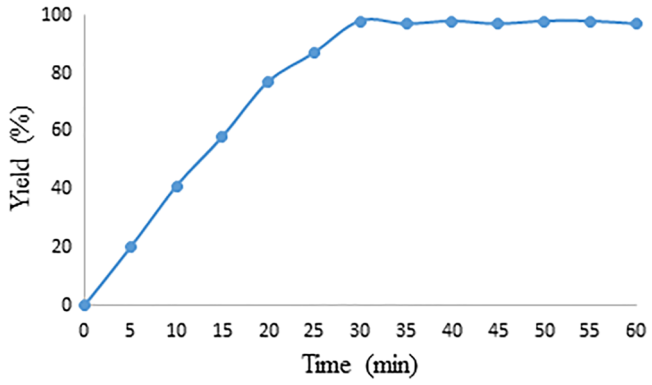

FIGURE 3 Effect of time on yield of tetrahydrodipyrazolo pyridines: ethyl acetoacetate (or diethylmalonate) (2 mmol), hydrazine hydrate (or phenyl hydrazine) (2.0 mmol), aromatic aldehyde (1.0 mmol) and ammonium acetate (4.0 mmol), Fe_3O_4@KCC-1-npr-NH_2 (0.1 gm), EtOH (5 ml), under reflux conditions for 30 min

TABLE 2 Influence of different nanocatalysts for the synthesis of tetrahydrodipyrazol pyridine

Entry	Catalyst	Yield (%)
1	KCC-1	-
2	KCC-1-npr-NH_2	-
3	Fe_3O_4	-
4	Fe_3O_4@KCC-1	-
5	Fe_3O_4@KCC-1-npr-NH_2	98

Reaction conditions: ethyl acetoacetate (or diethylmalonate) (2 mmol), hydrazine hydrate (or phenyl hydrazine) (2.0 mmol), aromatic aldehyde (1.0 mmol) and ammonium acetate (4.0 mmol), Fe3O4@ KCC-1-npr-NH2 (0.1 gm), EtOH (5 ml), under reflux conditions for 30 min. Isolated yield (%).

(or hydrazine hydrate), ethyl acetoacetate (or diethylmalonate), ammonium acetate, and a variety of different substituted aromatic aldehydes in the presence of Fe_3O_4@KCC-1-NH_2 MNP in ethanol under reflux conditions. As can be seen in Table 3, the type of substituents on the aromatic ring and electronic effects did not show extremely evident effects in terms of yields under the reaction conditions. Aromatic aldehydes containing electron-donating groups or electron-withdrawing and even without these groups wereused and reacted well to afford the desired tetrahydrodipyrazolo pyridines in excellent yields with high purity.

It is undeniable that for a catalytic process, the recovery and reuse of catalyst materials are highly preferable. In this regard, the recyclability of the Fe_3O_4@KCC-1-NH_2 MNP was investigated using the model reaction of phenyl hydrazine (or hydrazine hydrate), ethyl acetoacetate (or diethylmalonate), aromatic aldehydes and ammonium acetate under identical reaction conditions. After the completion of reaction, the recovered catalyst from the reaction mixture was washed with chloroform and dried at room temperature and reused for subsequent reactions. It is obviousthat the heterogeneous and magnetic property of the Fe_3O_4@KCC-1-NH_2 MNP facilitates the effective recovery of the nanocatalyst from the reaction mixture by external magnet during the work-up procedure so that the catalyst could be recycled and reused up to ten consecutive trialswithout remarkable loss of its catalytic activity (Figure 4a and 4b) after nine tests. Thus, these results indicated that the nanocatalyst was stable and could tolerate the multicomponent reaction conditions.

In this research, we also synthesized six new tetrahydrodipyrazolo pyridine derivatives according to the explained method in Scheme 1. Spectroscopic data:

3.1 | *4-(1H-indol-3-yl)-3,5-dimethyl-1,4,7,8-tetrahydrodipyrazolo[3,4-b:4′,3′-e] pyridine* (5a, $C_{17}H_{16}N_6$)

Orange solid; m.p.: >300 °C; FT-IR (KBr): ν_{max}/cm^{-1} 3250 (NH), 3058, 2917, 2827, 2761, 2394, 2280, 1804, 1750, 1680, 1510, 1475, 1345, 1240, 1160, 1005, 984, 751; ^{1}H NMR (400 MHz, DMSO-d_6): δ = 2.24 (s, 6H, CH_3), 4.94 (s, 1H, CH, Aliphatic), 7.26–7.28 (m, 2H, Ar), 7.55–7.58 (m, 2H, Ar), 7.92 (s, 1H, Ar), 9.75 (s, 1H, NH), 10.81 (s, 1H, NH), 11.03 (s, 1H, NH), 12.77 (s, 1H, NH) ppm; ^{13}C NMR (100 MHz, DMSO-d_6): δ = 10.31 (CH_3), 13.01 (CH_3), 23.08 (CH), 111.9, 112.7, 118.4, 118. 8, 121.6, 123.1, 135.1, 136.3, 136.9, 149.4, 166.3 ppm. Anal. Calcd for $C_{17}H_{16}N_6$. Calcd. C, 67.09; H, 5.30; N, 27.61. Found, C, 66.99; H, 5.27; N, 27.69%.

TABLE 3 Synthesis of tetrahydrodipyrazolo pyridines in the presence of the Fe_3O_4@KCC-1-npr-NH_2 catalyst in ethanol

Entry	Product No.	R	R′	R″	Product	Time (min)	Yield (%)	MP (°C) Found	MP (°C) Reported
1	5a	Me	H	1H-indole		30	90	>300	-
2	5b	Me	H	1,1′-biphenyl		30	92	280–282	-
3	5c	Me	Ph	1H-indole		30	95	245–247	-
4	5d	Me	Ph	1,1′-biphenyl		30	93	193–195	-
5	5e	Me	Ph	4-BrC_6H_4		20	96	>300	-
6	5f	OEt	Ph	1,1′-biphenyl		2	98	196–197	-
7	5 g	Me	H	Ph		30	92	238–239	237–239[40]
8	5 h	Me	H	4-ClC_6H_4		30	92	151–152	251–253[41]
9	5i	Me	H	4-FC_6H_4		30	91	260–261	258–260[40]
10	5j	Me	H	4-$NO_2C_6H_4$		30	97	>300	>300[40]
11	5 k	Me	H	4-$MeOC_6H_4$		30	87	182–184	181–183[40]
12	5 l	Me	H	4-MeC_6H_4		30	94	246–247	245–247[41]
13	5 m	Me	H	4-OHC_6H_4		30	90	269–270	269–271[40]

Reaction conditions: ethyl acetoacetate (or diethylmalonate) (2 mmol), hydrazine hydrate (or phenyl hydrazine) (2.0 mmol), aromatic aldehyde (1.0 mmol) and ammonium acetate (4.0 mmol), Fe3O4@ KCC-1-npr-NH2 (0.1 gm), EtOH (5 ml), under reflux conditions for 2–30 min. Isolated yield (%).

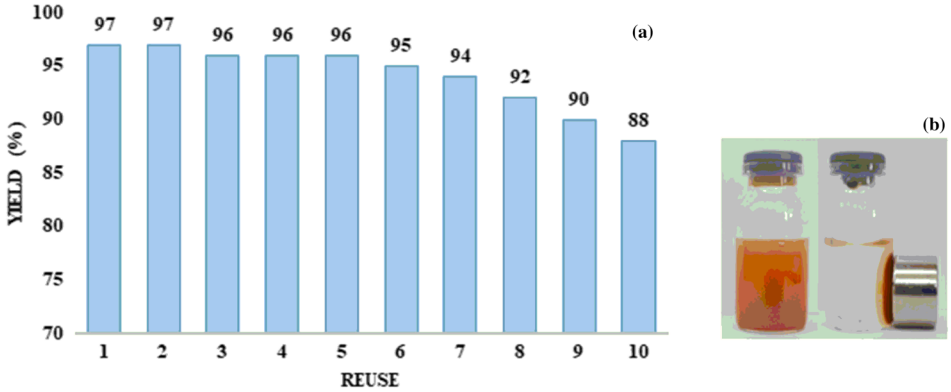

FIGURE 4 (a) Reusability of Fe_3O_4@ KCC-1-npr-NH_2 MNPCs and (b) separation of the nanocatalyst by external magnet

3.2 | 4-([1,1′-biphenyl]-4-yl)-3,5-dimethyl-1,4,7,8-tetrahydrodipyrazolo[3,4-b:4′,3′-e] pyridine (5b, $C_{21}H_{19}N_5$)

White solid; m.p.: 280–282 °C; FT-IR (KBr): ν_{max}/cm^{-1} 3590, 3500 (NH), 3378, 3050, 2907, 2850, 2214, 1980, 1650, 1600, 1570, 1505, 1460, 1405, 1370, 1230, 1005, 954, 812; ^1H NMR (400 MHz, DMSO-d_6): δ = 2.18 (s, 6H, CH_3), 4.84 (s, 1H, CH, Aliphatic), 7.22 (d, J = 8.01 Hz, 2H, PH), 7.31 (t, J = 7.22 Hz,1H, PH), 7.42 (t, J = 7.58 Hz, 2H, PH), 7.50 (d, J = 8.10 Hz, 2H, PH), 7.60 (d, J = 7.50 Hz, 2H, PH), 11.51 (b, 3H, NH) ppm; ^{13}C NMR (100 MHz, DMSO-d_6): δ = 10.37 (CH_3), 32.47 (CH), 104.21, 126.1, 126.4, 127.0, 128.0, 128.8, 137.4, 139.9, 140.2, 142.7, 161.2 ppm. Anal. Calcd for $C_{21}H_{19}N_5$. Calcd. C, 73.88; H, 5.61; N, 20.51. Found, C, 74.00; H, 5.58; N, 20.48%.

3.3 | *4-(1H-indol-3-yl)-3,5-dimethyl-1,7-diphenyl-1,4,7,8-tetrahydrodipyrazolo[3,4-b:4′,3′-e] pyridine* (5c, $C_{29}H_{24}N_6$)

Orange solid; m.p.: 245–247 °C; FT-IR (KBr): ν_{max}/cm^{-1} 3750, 3500 (NH), 3200, 3007, 2950, 2904, 2870, 2300, 2280, 1690, 1646, 1600, 1475, 1390, 1376, 1358, 1200, 1103, 1002, 850, 795; ^1H NMR (400 MHz, DMSO-d_6): δ = 2.41 (s, 6H, CH_3), 4.12 (s, 1H, CH, Aliphatic), 7.16–7.69 (10H, Ar), 8.00–8.16 (6H, Ar), 9.8 (s, 1H, NH), 12.6 (s, 1H, NH) ppm; ^{13}C NMR (100 MHz, DMSO-d_6): δ = 13.0 (CH_3), 28.47 (CH), 112.2, 112.9, 118.0, 118.3, 118.6, 122.1, 123.5, 123.9, 128.1, 128.6, 136.4, 137.2, 138.2, 138.9, 150.9, 162.8 ppm. Anal. Calcd for $C_{29}H_{24}N_6$. Calcd. C, 76.29; H, 5.30; N, 18.41. Found, C, 76.20; H, 5.25; N, 18.45%.

3.4 | *4-([1,1′-biphenyl]-4-yl)-3,5-dimethyl-1,7-diphenyl-1,4,7,8-tetrahydrodipyrazolo[3,4-b:4′,3′-e] pyridine* (5d, $C_{33}H_{27}N_5$)

White solid; m.p.: 193–195 °C; FT-IR (KBr): ν_{max}/cm^{-1} 3760, 3400 (NH), 2960, 2850, 2280, 2904, 2870, 2300, 2280, 1800, 1686, 1530, 1475, 1290, 1100, 1001, 853; ^1H NMR (400 MHz, DMSO-d_6): δ = 2.35 (s, 6H, CH_3), 5.01 (s, 1H, CH, Aliphatic), 7.25–7.73 (m, 19 H, Ar), 14.04 (s, 1H, NH) ppm; ^{13}C NMR (100 MHz, DMSO-d_6): δ = 11.61 (CH_3), 28.14 (CH), 120.5, 125.5, 126.5, 127.7, 128.8, 142.13, 146.2, 150.3 ppm. Anal. Calcd for $C_{33}H_{27}N_5$. Calcd. C, 80.30; H, 5.51; N, 14.19. Found, C, 81.01; H, 5.47; N, 14.21%.

3.5 | *4-(4-bromophenyl)-3,5-dimethyl-1,7-diphenyl-1,4,7,8-tetrahydrodipyrazolo[3,4-b:4′,3′-e] pyridine* (5e, $C_{27}H_{22}BrN_5$)

Yellow solid; m.p.: >300 °C; 3760, FT-IR (KBr): ν_{max}/cm^{-1} 3400 (NH), 2962, 2900, 2380, 2304, 1800, 1686, 1530, 1475, 1160, 880, 1001, 720, 660 (C-Br); ^1H NMR (400 MHz, DMSO-d_6): δ = 2.35 (s, 6H, CH_3), 5.13 (s, 1H, CH, Aliphatic), 7.24 (t, J = 6.72 Hz, 2H, Ar), 7.44 (t, J = 7.42 Hz,4H, Ar), 7.52 (d, J = 8.21 Hz, 2H, Ar), 7.71 (d, J = 7.72 Hz, 4H, Ar), 8.17 (d, J = 8.30 Hz, 2H, Ar), 13.88 (s, 1H, NH) ppm; ^{13}C NMR (100 MHz, DMSO-d_6): δ = 11.56 (CH_3), 33.20 (CH), 103.8, 120.5, 123.3, 125.6, 128.5, 128.9,137.1, 145.9, 146.2, 150.3 ppm. Anal. Calcd for $C_{27}H_{22}BrN_5$. Calcd. C, 65.33; H, 4.47; Br, 16.10; N, 14.11. Found, C, 65.25; H, 4.45; Br, 16.17; N, 14.08%.

3.6 | *4-([1,1′-biphenyl]-4-yl)-1,7-diphenyl-1,4,7,8-tetrahydrodipyrazolo[3,4-b:4′,3′-e] pyridine-3,5-diol* (5f, $C_{31}H_{23}N_5O_2$)

White solid; m.p.: 196–197 °C; FT-IR (KBr): ν_{max}/cm^{-1} 3720, 3500 (NH), 3995 (OH), 3370, 3180, 3004, 2900, 2806, 2390, 2300, 2260, 1880, 1701, 1670, 1560, 1501, 1450, 1400, 1210, 1140, 1100, 900, 820, 800, 756; ^1H NMR (400 MHz, DMSO-d_6): δ = 4.18 (s, 1H, CH, Aliphatic), 6.76 (t, J = 7.06, 1H, Ar), 7.12 (d, J = 7.8, 2H, Ar), 7.24 (t, J = 7.5, 2H, Ar), 7.35 (t, J = 7.1, 1H, Ar), 7.46 (t, J = 7.5, 2H, Ar), 7,68–7.75 (m, 6H, Ar), 7.92 (s, 1H, OH), 10.43 (s, 1H, NH) ppm; ^{13}C NMR (100 MHz, DMSO-d_6): δ =112.0, 118.8, 126.1, 126.4, 126.8, 127.4, 128.9, 129.1, 135.0, 135.9, 139.3, 139.6, 145.2 ppm. Anal. Calcd for $C_{35}H_{31}N_5O_2$. Calcd. C, 74.83; H, 4.66; N, 14.08; O, 6.43 Found, C, 73.99; H, 4.63; N, 14.12; O, 6.39%.

3.7 | Biological studies

After implementation the synthesis of tetrahydrodipyrazolopyridines noted in Table 3, the prepared novel tetrahydrodipyrazolopyridines (5a-5f) were tested for in vitro cytotoxicity analyses against two different cancer cell lines; human breast adenocarcinoma (MCF 7) and human colon adenocarcinoma (HT 29) using the MTT assay.[36] Also doxorubicin, a well-known anticancer agent, was used as the positive control in our study. The antiproliferaty efficacy records are presented as IC_{50} values described as the concentration of the product that reduces cell proliferation at 50% (Table 4). The IC_{50} values for cell lines were determined after at least three individual experiments. Cell survival was ascertained by MTT assay as explained in methods and materials subsection.

3.8 | Cytotoxicity evaluation and the structure activity relationships study

Novel synthetic tetrahydrodipyrazolopyridines (5a-f) were investigated on cytotoxicity effects and some of them showed interesting results. The results proved that derivatives 5a, 5c and 5 f possessed considerable activity against two cell lines (Table 4). The compound 5e exhibited promising activities against MCF7 cell line, while compound 5b against HT 29 cell line. During this bioevaluation, 5c, 5 f and 5a have been recognized as the most active products against MCF-7 and HT-29 cell lines, respectively. It has been clear that the tetrahydrodipyrazolopyridines containing indole (5c and 5a) and hydroxide (5f) moieties showed impressive cytotoxic activity also these mentions compounds were found to be more active among all synthetic compounds. In our study, all the synthetic compounds were found to have cytotoxic properties and any of these compounds were

TABLE 4 IC_{50} (μM) of the synthesized compounds against different cancer cell lines

		IC50 values (in μM)	
Entry	**Sample Code**	**MFC 7**	**HT 29**
1	5a	8	8
2	5b	50	75
3	5c	2.5	2.5
4	5d	10	12
5	5e	60	35
6	5f	5	4.5
STD	Doxorubicin	2.4 ± 0.12	0.49

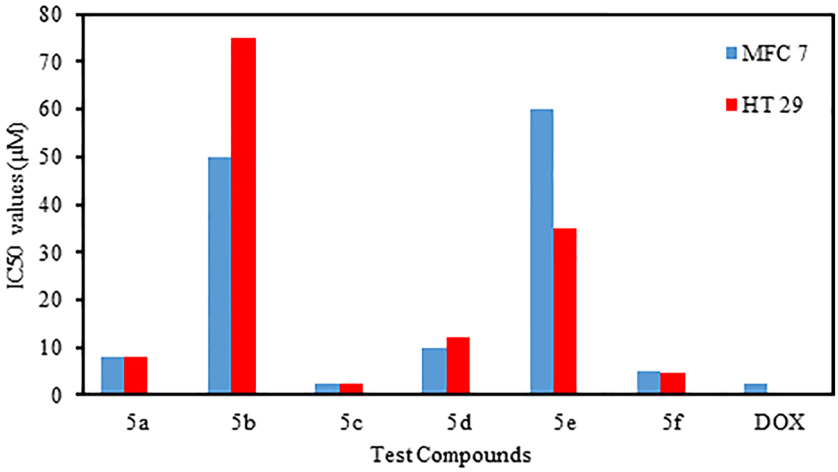

FIGURE 5 Graphical presentation of the cytotoxic activity of the tetrahydrodipyrazolopyridines

not inactive. In addition, the existence of a heterocyclic moiety (5c and 5a) enhanced the cytotoxic properties against MCF-7 and HT-29 cell lines. However, a tetrahydrodipyrazolopyridines containing an aromatic ring without an electron-withdrawing or even electron-donating group (as for example, in 5b and 5d except 5 f) was found to have less cytotoxic activities. Although the compound with bromide (5e) moiety was also low active against HT-29 cell line. The cytotoxic activity of all the terahydrodipyrazolopyridines has been graphically exhibited in Figure 5.

It is important to point out that, the multicomponent reactions were also be utilized for synthesis of functional polymers and composites.[42–51]

4 | CONCLUSIONS

In summary, a novel magnetic nanocatalyst (Fe_3O_4@KCC-1-nPr-NH_2) was prospered and used for the synthesis of tetrahydrodipyrazolo pyridine derivatives in ethanol as a solvent in excellent yield under reflux reaction condition. This nanocatalyst could be recovered and reused at least ten times with no decrease in its activity and selectivity. Proposed method has some advantages containing short reaction times, mild reaction conditions, reusability of the solid catalyst, high yields and convenient workup process. The anticancer activities of novel tetrahydrodipyrazolo pyridine derivatives was also investigated. MTT assay exhibited that all synthetic products have shown significant cytotoxicity activity. Moreover, evaluation of anticancer activity revealed that some of these compounds have good cytotoxic activity against one or two cancer cell lines.

ACKNOWLEDGEMENTS

This Research was supported by Tabriz University and Tabriz University of Medical Sciences.

CONFLICT OF INTEREST

No potential conflict of interest was reported by the authors.

ORCID

Mohammad Hasanzadeh https://orcid.org/0000-0003-4918-1239

REFERENCES

[1] C. Samar, A. Ismail, T. Helmi, J. Khiari, J. Bassem, *J. Bacteriol. Parasitol.* **2017**, *8*, 1.
[2] T. Maqbool, A. Nazeer, M. N. Khan, M. C. Elliott, M. A. Khan, M. Ashraf, M. Nasrullah, S. Arshad, M. A. Munawar, *Asian J. Chem.* **2014**, *26*, 2870.
[3] M. S. Salem, M. A. M. Ali, *Biol. Pharm. Bull.* **2016**, *39*, 473.
[4] J. Sindhu, H. Singh, J. Khurana, J. K. Bhardwaj, P. Saraf, C. Sharma, *Med. Chem. Res.* **2016**, *25*, 1813.
[5] J. Quiroga, Y. Villarreal, J. Gálvez, A. Ortíz, B. Insuasty, R. Abonia, M. Raimondi, S. Zacchino, *Chem. Pharm. Bull.* **2017**, *65*, 143.
[6] N. R. Mohamed, N. Y. Khaireldin, A. Fahmyb, A. El-Sayeda, *Der. Pharm. Chem.* **2010**, *2*, 400.
[7] K. S. Gudmundsson, B. A. Johns, S. H. Allen, *Bioorg. Med. Chem. Lett.* **2008**, *18*, 1157.
[8] H. de Mello, A. Echevarria, A. M. Bernardino, M. Canto-Cavalheiro, L. L. Leon, *J. Med. Chem.* **2004**, *47*, 5427.
[9] N. C. Warshakoon, S. Wu, A. Boyer, R. Kawamoto, S. Renock, K. Xu, M. Pokross, A. G. Evdokimov, S. Zhou, C. Winter, *Bioorg. Med. Chem. Lett.* **2006**, *16*, 5687.
[10] S. Wenglowsky, D. Moreno, J. Rudolph, Y. Ran, K. A. Ahrendt, A. Arrigo, B. Colson, S. L. Gloor, G. Hastings, *Bioorg. Med. Chem. Lett.* **2012**, *22*, 912.
[11] M. Chioua, A. Samadi, E. Soriano, O. Lozach, L. Meijer, J. Marco-Contelles, *Bioorg. Med. Chem. Lett.* **2009**, *19*, 4566.
[12] C. J. Mitchell, S. P. Ballantine, D. M. Coe, C. M. Cook, C. J. Delves, M. D. Dowle, C. D. Edlin, J. N. Hamblin, S. Holman, M. R. Johnson, *Bioorg. Med. Chem. Lett.* **2010**, *20*, 5803.
[13] N. Tschammer, J. Elsner, A. Goetz, K. Ehrlich, S. Schuster, M. Ruberg, J. Kühhorn, D. Thompson, J. Whistler, H. Hübner, *J. Med. Chem.* **2011**, *54*, 2477.

[14] I. H. Eissa, A. M. El-Naggar, M. A. El-Hashash, *Bioorg. Chem.* **2016**, *67*, 43.
[15] J. S. Ghomi, S. Kalhor, H. Shahbazi-Alavi, M. Asgari-Kheirabadi, *Turk. J. Chem.* **2015**, *39*, 843.
[16] V. Estevez, M. Villacampa, J. C. Menendez, *Chem. Soc. Rev.* **2010**, *39*, 4402.
[17] A. Ghaedi, G. Bardajee, A. Mirshokrayi, M. Mahdavi, A. Shafiee, T. Akbarzadeh, *RSC Adv.* **2015**, *5*, 89652.
[18] Z. Chen, Y. Shi, Q. Shen, H. Xu, F. Zhang, *Tetrahedron Lett.* **2015**, *56*, 4749.
[19] H. Singh Sohal, M. Kaur, R. Khare, K. Singh, *Am. J. Org. Chem.* **2014**, *4*, 21.
[20] P. Gunasekaran, P. Prasanna, S. Perumal, *Tetrahedron Lett.* **2014**, *55*, 329.
[21] S. Santra, M. Rahman, A. Roy, A. Majee, A. Hajra, *Catal. Commun.* **2014**, *49*, 52.
[22] A. Mobaraki, B. Movassagh, B. Karimi, *Appl. Catal., a* **2014**, *472*, 123.
[23] N. Koukabi, E. Kolvari, A. Khazaei, M. A. Zolfigol, B. Shirmardi-Shaghasemi, H. R. Khavasi, *Chem. Commun.* **2011**, *47*, 9230.
[24] D. Zhang, C. Zhou, Z. Sun, L.-Z. Wu, C.-H. Tung, T. Zhang, *Nanoscale* **2012**, *4*, 6244.
[25] F. A. Tameh, J. Safaei-Ghomi, M. Mahmoudi-Hashemi, H. Shahbazi-Alavi, *RSC Adv.* **2016**, *6*, 74802.
[26] J. Safaei-Ghomi, H. Shahbazi-Alavi, *Scientia Iranica. Trans. C Chem. Chem. Eng.* **2017**, *24*, 1209.
[27] S. Shylesh, V. Schünemann, W. R. Thiel, *Angew. Chem. Int. Ed.* **2010**, *49*, 3428.
[28] J. G. Huddleston, A. E. Visser, W. M. Reichert, H. D. Willauer, G. A. Broker, R. D. Rogers, *Green Chem.* **2001**, *3*, 156.
[29] M. A. El-Borai, H. F. Rizk, D. M. Beltagy, I. Y. El-Deeb, *Eur. J. Med. Chem.* **2013**, *66*, 415.
[30] S. Abu-Melha, *Arch. Pharm.* **2013**, *346*, 912.
[31] J. A. Pfefferkorn, M. Tu, K. J. Filipski, A. Guzman-Perez, J. Bian, G. E. Aspnes, M. F. Sammons, W. Song, J.-C. Li, C. S. Jones, *Bioorg. Med. Chem. Lett.* **2012**, *22*, 7100.
[32] J. Safaei-Ghomi, R. Sadeghzadeh, H. Shahbazi-Alavi, *RSC Adv.* **2016**, *6*, 33676.
[33] J. Soleymani, M. Hasanzadeh, M. H. Somi, N. Shadjou, A. Jouyban, *Biosens. Bioelectron.* **2019**, *132*, 122.
[34] B. Singh, V. Polshettiwar, *J. Mater. Chem. A* **2016**, *4*, 7005.
[35] Q. Yue, Y. Zhang, C. Wang, X. Wang, Z. Sun, X.-F. Hou, D. Zhao, Y. Deng, *J. Mater. Chem. A* **2015**, *3*, 4586.
[36] Z. Ghasemi, S. Azizi, R. Salehi, H. S. Kafil, *Monatsh. Chem. Chem. Mon.* **2018**, *149*, 149.
[37] Y. Wang, X. Peng, J. Shi, X. Tang, J. Jiang, W. Liu, *Nanoscale Res. Lett.* **2012**, *7*, 86.
[38] N. Bayal, B. Singh, R. Singh, V. Polshettiwar, *Sci. Rep.* **2016**, *6*, 24888.
[39] K. AbouAitah, A. Swiderska-Sroda, A. A. Farghali, J. Wojnarowicz, A. Stefanek, S. Gierlotka, A. Opalinska, A. K. Allayeh, T. Ciach, W. Lojkowski, *Oncotarget* **2018**, *9*, 26466.
[40] K. Zhao, M. Lei, L. Ma, L. Hu, *Monatsh. Chem. Chem. Mon.* **2011**, *142*, 1169.
[41] M. Dabiri, P. Salehi, M. Koohshari, Z. Hajizadeh, D. I. MaGee, *ARKIVOC* **2014**, *5*, 204.
[42] Z. Long, L. Mao, M. Liu, Q. Wan, Y. Wan, X. Zhang, Y. Wei, *Polym. Chem.* **2017**, *8*, 5644.
[43] L. Mao, Y. Liu, S. Yang, Y. Li, X. Zhang, Y. Wei, *Dyes Pigm.* **2019**, *162*, 611.
[44] R. Jiang, M. Liu, T. Chen, H. Huang, J. Tian, Y. Wen, Q. Cao, X. Zhang, Y. Wei, *Dyes Pigm.* **2018**, *148*, 52.
[45] R. Jiang, H. Liu, M. Liu, J. Tian, Q. Huang, H. Huang, Y. Wen, Q. Y. Cao, X. Zhang, Y. Wei, *Mater. Sci. Eng. C* **2017**, *81*, 416.
[46] R. Jiang, H. Liu, M. Liu, J. Tian, Q. Huang, H. Huang, Y. Wen, Q. Y. Cao, X. Zhang, Y. Wei, *Mater. Sci. Eng. C* **2017**, *80*, 708.
[47] Q. Y. Cao, R. Jiang, H. Liu, M. Liu, J. Tian, Q. Huang, H. Huang, Y. Wen, X. Zhang, Y. Wei, *Mater. Sci. Eng. C* **2017**, *80*, 411.
[48] Y. Liu, L. Mao, X. Liu, M. Liu, D. Xu, R. Jiang, F. Deng, Y. Li, X. Zhang, Y. Wei, *Mater. Sci. Eng. C* **2017**, *79*, 590.
[49] Q. Huang, M. Liu, J. Zhao, J. Chen, G. Zeng, H. Huang, J. Tian, Y. Wen, X. Zhang, Y. Wei, *Appl. Surf. Sci.* **2018**, *427*, 535.
[50] J. Dou, D. Gan, Q. Huang, M. Liu, J. Chen, F. Deng, X. Zhu, Y. Wen, X. Zhang, Y. Wei, *Int. J. Biol. Macromol.* **2019**, *136*, 476.
[51] Q. Huang, M. Liu, J. Chen, F. Deng, X. Zhu, Y. Wen, X. Zhang, Y. Wei, *J. Colloid Interface Sci.* **2017**, *499*, 170.

SUPPORTING INFORMATION

Additional supporting information may be found online in the Supporting Information section at the end of this article.

How to cite this article: Azizi S, Soleymani J, Hasanzadeh M. Iron oxide magnetic nanoparticles supported on amino propyl-functionalized KCC-1 as robust recyclable catalyst for one pot and green synthesis of tetrahydrodipyrazolopyridines and cytotoxicity evaluation. *Appl Organometal Chem*. 2020;e5440. https://doi.org/10.1002/aoc.5440